IJE TRANSACTIONS A: Basics Vol. 35, No. 07, (July 2022) 1343-1354

International Journal of Engineering

Journal Homepage: www.ije.ir

Collision-free Inverse Kinematics of Redundant Manipulator for Agricultural Applications through Optimization Techniques

A. Sridhar Reddy*[a], V. V. M. J. Satish Chembuly[b], V. V. S. Kesava Rao[a]

[a] *Department of Mechanical Engineering, College of Engineering (A), Andhra University, Visakhapatnam, India*
[b] *Department of Mechanical Engineering, Aditya College of Engineering and Technology, Surampalem, India*

PAPER INFO

Paper history:
Received 29 January 2022
Received in revised form 16 March 2022
Accepted 12 April 2022

Keywords:
Agricultural Robot
Redundant Manipulator
Inverse Kinematics
Optimization
Obstacle Avoidance
Simscape Multibody

ABSTRACT

This article presents an optimization-based technique for solving the *inverse kinematics* (IK) of spatially redundant manipulators in agricultural environments (workspaces). A kinematic configuration of 9 *degrees of freedom* (DOF) manipulator with eight revolute and one prismatic joint has been modelled to improve the accessibility in complex workspaces. The proposed manipulator has been simulated for harvesting fruits and vegetables. To perform the desired task in the working environment, the IK solution of the robot needs to be determined. The IK problem has been formulated as a constrained optimization problem with the objective of minimizing the positional and orientational errors by avoiding obstacles. A 3D CAD environment with different fruits and vegetable plants has been modelled in Solidworks. A target location in this environment has been chosen to pluck the fruit/vegetables. The trunk, branches, and leaves are considered as obstructions. The collision avoidance technique was implemented using a bounding box approach by including a collision detection algorithm. IK simulations of the spatial redundant manipulator in a cluttered environment were performed and results are reported. The joint trajectories of the robot while reaching desired task-space location has been depicted using Simscape Multibody. The results demonstrate that the end-effector of the robot has been reached desired task location successfully with an accurate IK solution. The approach is adaptable in a wide range of working environments based on the simulation results of the IK solution of robots.

doi: *10.5829/ije.2022.35.07a.13*

NOMENCLATURE

IK	Inverse kinematics	URDF	Unified Robotic Description Format
DOF	Degrees of freedom	P_{error}	Positional error
CAD	Computer aided design	O_{error}	Orientational error
2D, 3D	Two, Three dimensional	f	Minimization function
a	Link length	**Greek Symbols**	
d	Join offset	α	Link twist
l_i	Length of the ith link	θ	Joint angle
C_i	Penalty for ith iteration	$(\alpha_d, \beta_d, \gamma_d)$	Desired orientation of end effector in Euler angles
q_i	Joint variable for ith joint	$(\alpha_a, \beta_a, \gamma_a)$	Actual orientation of end effector in Euler angles
SQP	Sequential Quadratic Programming	**Subscripts**	
R^2	Correlation coefficient	i	Link number
D–H	Denavit– Hartenberg	l	Lower bound
slx	Simulink model data format	u	Upper bound

*Corresponding Author Institutional Email: asridhareddy@andhrauniversity.edu.in (A. Sridhar Reddy)

Please cite this article as: A. Sridhar Reddy, V. V. M. J. Satish Chembuly, V. V. S. Kesava Rao, Collision-free Inverse Kinematics of Redundant Manipulator for Agricultural Applications through Optimization Techniques, ***International Journal of Engineering, Transactions A: Basics***, Vol. 35, No. 07, (2022) 1343-1354

1. INTRODUCTION

During the cultivation of bulk commodity crops like wheat, rice, and sugarcane, the tractor and combine harvester has virtually replaced the need for manual labor. Despite recent advances in agricultural automation, high-value specialty crops such as fruits and vegetables, horticulture, and nursery crops still rely mostly on labour. A large seasonal workforce is needed to produce a fresh market of fruits like guava and apples. Harvesting is a time-sensitive activity, with unpredictable weather patterns producing uncertainty when organizing employment [1]. When harvesting individual fruits and vegetables in horticulture and greenhouses, robots are required to identify the task space location. For these applications, reaching the desired task location by avoiding tree trunks, branches, and leaves remains challenging with respect to robot manipulation. Agricultural robots need to be perceptive and intelligent that are programmed to conduct a wide range of operations such as transplanting, cultivating, spraying, pruning, and harvesting [2] in a complex environment. Pedersen et al. [3] focused on the economic feasibility for applying autonomous robotic systems compared to conventional systems in different applications of cultivation. The use of robotic systems in agricultural applications seems more economically feasible than conventional harvesting equipment based on the conclusions drawn. By considering the profitable usage of robots in agriculture, Belforte et al. [4] designed and built a 3 DOF robot for spraying and precision fertilization applications.

Because of high crop harvesting expenses, researchers are concerned about the utilization of robots in the agricultural environment. In the twentieth century, technical developments in agricultural mechanization profoundly altered the structure of modern agriculture [5]. Bechar and Vigneault [6] presented a review on the design and development of agricultural robots along with associated principles and limitations. Selective harvesting is a challenging task for robots due to high levels of variation in objects, environmental, cultivation system, and task variation as well as incomplete information of the environment, noisy data from sensors. Kootstra et al. [7] discussed the current state of selective harvesting of apple, tomatoes, and broccoli in greenhouse, orchard, and open-field conditions. Perception, the complexity of the environment, task variation, operational speed, and safety are some of the critical components for harvesting robots.

From the literature, it has been noted that robots have been widely used in different harvesting applications. In such cases, the robot manipulator should be flexible enough to access the desired location. Because of its greater flexibility and maneuverability within a complex environment, it requires more DOF than is needed to accomplish the given task. These robots are kinematically redundant in nature. The excess DOF of the robot manipulator enables to reach the desired task location by avoiding the obstacles in the workspace [8].

In *Inverse Kinematics* (IK) [9], all possible sets of joint angles can be calculated, which could be used to attain the given position and orientation of the end-effector. This problem can be solved either analytically or numerically [10]. In an analytical approach, the solution can be obtained as a closed-form, and these solutions are desirable because they are faster than numerical solutions; however, such a solution is inherently dependent on the DOF of a manipulator. In the numerical approach, the solution can be obtained by iterative methods and these solutions are computationally effective even with an increase in the number of DOF. Aristidou and Lasenby [11] reviewed Jacobian Inverse methods (Pseudo-inverse, transpose, singular value decomposition, Damped least square, pseudo-inverse Damped least squares, and so on), Newton Methods, Sequential Monte Carlo methods, and Heuristic IK algorithms for solving IK problems numerically. A new heuristic IK methodology *'Forward and Backward Reaching Inverse Kinematics'* (FABRIK) was proposed by Aristidou and Lasenby [11].

In the literature, some of the researchers conducted several studies on IK methods using optimization techniques. Goldenberg and Lawrence [12] proposed a constrained optimization technique-based algorithm for redundant axes manipulators to obtain restrictive motion and to select a solution when multiple solutions exist. Kumar et al. [13] considered a 7 DOF (PA-10) manipulator for the IK solution and formulated it as a nonlinear optimization problem with the objective of energy minimization, for smooth tracking of the desired path. Bagheri et al. [14] acquired the IK solutions for 6 DOF robot by applying neural networks.

Many researchers solved the IK problem by considering joint level velocities by calculating the pseudo inverse of Jacobian [15]. These are sensitive at the singular configuration, also increasing the computational cost. An optimization-based approach for solving the IK problem of a planar redundant manipulator to avoid obstacles and singularities was implemented at a joint position level by avoiding the use of inverse of Jacobian, which is computationally effective [16].

In agricultural environments, the robot must be able to identify the task-space and obstacles in the environment in order to move around for harvesting purposes. As a result, obstacle detection becomes a major issue when harvesting robots are involved. To capture workspace coordinates vision sensors are needed. Vision sensors can be *two-dimensional* (2D) visual sensors or *three-dimensional* (3D) visual sensors. A monocular vision system is a 2D visual sensor type, that contains a single camera. It is used to detect fruit/vegetable in the

field. These sensors can be *Charge Coupled Device* (CCD) or *Complementary Metal Oxide Semiconductor* (CMOS). A binocular stereo-vision system is a 3D visual sensor, consisting of two cameras separated with some distance. The 3D map of fruit/vegetable can be obtained by the triangulation method [17]. Hartley and Sturm [18] developed an algorithm for the Triangulation problem to get the optimal global solution used to find the location of an object. van Henten et al. [19] used CCD as a vision sensor during the harvesting of cucumbers. A binocular stereo-vision system is mounted on Agrobot to identify the ripe tomato by Buemi et al. [20]. By capturing the images of the real-time environment, the coordinates of the workspace have been determined in the present work.

A virtual workspace with fruits and vegetables has been modelled, which resembles a real-time environment, and the dimensions are similar to the images that are taken. After creating the 3D map of the environment, the robot manipulator needs to reach the task-space (for fruit picking) location by avoiding the collision with obstacles (tree trunk, stems, etc.). Collision avoidance plays a pivotal role in motion planning and the IK of robot manipulators. A wide variety of techniques have been adopted for collision avoidance. Potential field methods are widely used obstacle avoidance techniques for mobile robots and manipulators. Khatib [21] proposed an artificial potential field method for obstacle avoidance. In this approach, obstacles exert repulsive forces, and the goal exerts an attractive force on the robot end-effector, from these, resultant force determines the direction of travel. Korayem et al. [22] presented a methodology for collision-free trajectory planning of mobile manipulators in cluttered environments based on potential field functions. Here, the mobile manipulator parts and environmental obstacles are modeled as ellipsoidal bodies. Based on the dynamic distance between colliding objects, Korayem et al. [23] formulated a dynamic potential function for tracking moving targets in dynamic environments for mobile manipulators. Potential field functions are also employed for collision avoidance during the motion planning of non-holonomic mobile robots in a cluttered environment [24]. Tang et al. [25] proposed an improved mathematical model of the APF (artificial potential field) method for the motion planning algorithm of citrus-picking robots. While the potential field principle is attractive due to its elegance and simplicity, however, it has significant problems of trapping at local minima, no passage between closely spaced obstacles, causing unstable motion in the presence of obstacles, and oscillations in narrow passages [26]. Gottschalk et al. [27] proposed an algorithm by placing a tight-fitting *oriented bounding box* (OBB) around a collection of polygons and grouping them into a tree hierarchy. This algorithm traverses two such trees and tests for overlaps based on the separating axis theorem. This algorithm takes a long time for parallel close proximity scenarios. Barequet and Har-Peled [28] discussed an algorithm for approximating the minimum-volume bounding box for 3-dimensional point sets, but this was not suitable for ellipsoidal point sets. Held et al. [29] used tetrahedron geometric primitive for generating bounding volume. But it does not fit tightly for many of the objects. This algorithm has to be recomputed if the orientation of the object is changed. Chembuly and Voruganti [30] implemented a classical constrained optimization technique to perform inverse kinematics of hyper redundant manipulator along with collision avoidance algorithm. Here, the boundaries of obstacles are enveloped by a 3D bounding box. A set of points are taken on the manipulator, when these point coordinates are inside the bounding box, a collision was detected.

Bac et al. [31] conducted a study on harversting robots, and reported that the algorithms available for obstacle localization, task planning, and motion planning are very limited. Tinoco et al. [32] pointed out the need for path planning and collision avoidance algorithms for agricultural applications. From the literature, it is observed that most of the IK solution and Collision avoidance techniques implemented for agricultural applications are computationally expensive and difficult for solving. Hence, there is a need for robots in agricultural applications, which can travel through narrow regions to spray the pesticides and/or to pick the fruits/vegetables by avoiding the collision with surrounding tree branches, which motivates study on agricultural robots. This paper proposed a redundant manipulator to access the task-space location in any direction. IK for the redundant manipulator was computed by considering it as an optimization problem to reduce the computational burden. Incorporating a collision detection algorithm into the bounding box approach can help to eliminate robot collisions with surrounding objects.

This paper is structured as follows. In section 2 discussion on harvesting robot. Section 3 describes the collision detection technique. Section 4 describes the optimization and problem formulation; then the results and discussion in section 5 and finally with conclusions.

2. HARVESTING ROBOT

2. 1. Manipulator Requirements In the present study, the trellis for agricultural plantations is positioned at 1000 mm from the ground. Fruits of guava trees grow 500 mm to 1200 mm above the ground. A 9DOF manipulator with 1P8R configuration was selected based on the requirements. A prismatic joint is selected for accessing large displacement in the vertical direction. The last 3 DOF of the manipulator constitutes wrist, which allows a roll-pitch-yaw motion for the end-effector.

2. 2. Kinematic Model Kinematic modeling is the basis for trajectory planning and control. The Denavit–Hartenberg approach is used to analyze forward kinematics the robot Parameters can be specified to build the coordinate relationship between adjacent joints.

The assignment of coordinate frames at the robot joints is the first step in the forward kinematic analysis, and these frames are used to determine the location and orientation of one frame relative to another frame. Redundant manipulator frame assignment is depicted in Figure 1(a), the robot configuration for the proposed work is modeled using Solidworks, shown in Figure 1(b). Conventional D–H parameters are provided for the frames and listed in Table 1.

The transformation of the frame (i) relative to the previous frame $(i-1)$ is derived from a generalized homogeneous transformation matrix, given in Equation (1)

$$ {}^{i-1}_{i}T = \begin{bmatrix} \cos\theta_i & -\sin\theta_i\cos\alpha_i & \sin\theta_i\sin\alpha_i & a_i\cos\theta_i \\ \sin\theta_i & \cos\theta_i\cos\alpha_i & -\cos\theta_i\sin\alpha_i & a_i\sin\theta_i \\ 0 & \sin\alpha_i & \cos\alpha_i & d_i \\ 0 & 0 & 0 & 1 \end{bmatrix} \quad (1) $$

For the serial manipulator shown in Figure 1(b), the end-effector's final location relative to the base frame is given by:

$$ {}^{0}_{9}T = {}^{0}_{1}T\,{}^{1}_{2}T\,{}^{2}_{3}T\,{}^{3}_{4}T\,{}^{4}_{5}T\,{}^{5}_{6}T\,{}^{6}_{7}T\,{}^{7}_{8}T\,{}^{8}_{9}T \quad (2) $$

Using the homogeneous transformation matrix Equation (2), the end-effector position and orientation can be determined.

2. 3. Object Identification in the Environment In the agricultural field, images are taken in different directions of views for locating the object (fruit/vegetables). The coordinates of the object can be determined by using the 'mapping technique' [33]. This technique requires some data points from the image to map with real-world coordinates.

For this purpose, four random locations are identified in the field and their distance is measured from the reference point. Then the images were taken, the pixels at target locations can be mapped with actual distances using Matlab image processing toolbox.

Actual measured distances vs. image pixels are summarized in Table 2, and a quadratic polynomial curve was fitted as shown Figure 2 and Equation (3) which has a correlation coefficient (R^2) equal to 0.9995. The correlation coefficient near one represents the best-fitted curve. So, this regression equation is further used to find the real-world coordinates from the image data.

$$ y = 0.0667x^2 - 24.664x + 2546.5 \quad (3) $$

where x is data from the image, y is the location of the object in the real-world coordinate system.

Figure 3 shows the distance measurement in the Bitter gourd field using the *Image processing toolbox*.

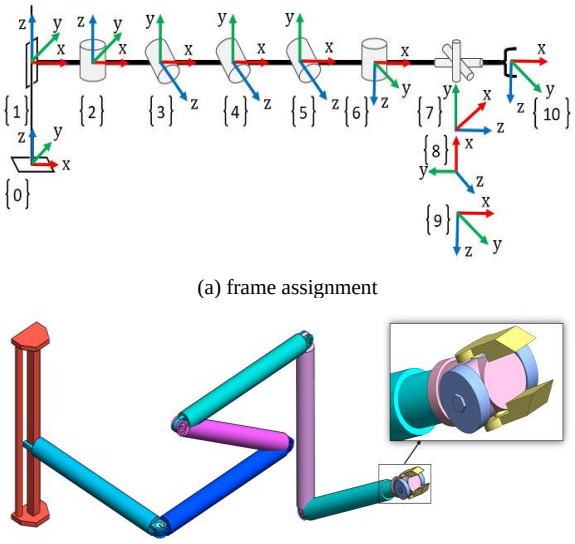

(a) frame assignment

(b) Solidworks 3D model

Figure 1. Redundant Manipulator

TABLE 1. D-H parameters

link	α	a	θ	d
1	0	l_1	0	d_1
2	90	L_2	0	0
3	0	L_3	0	0
4	0	L_4	0	0
5	90	L_5	0	0
6	-90	l_6	-90	0
7	-90	0	90	0
8	90	0	-90	0
9	0	0	0	0

TABLE 2. Image vs. field measured data

S. No.	Measurement	
	Image (pixel)	Field (mm)
1	202	280
2	214	330
3	253	570
4	280	870

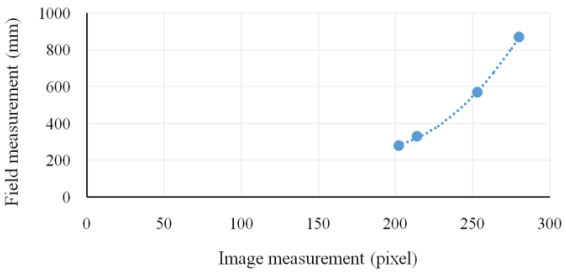

Figure 2. Polynomial curve fitting for image mapping

(a) Image from front

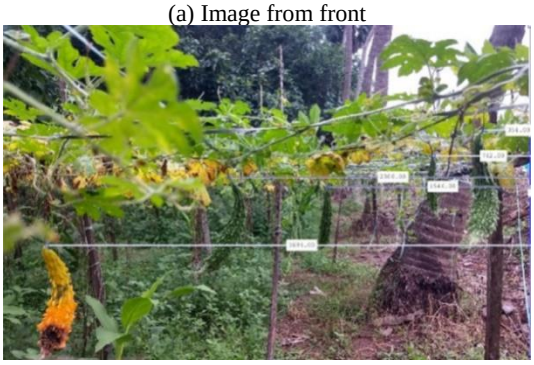

(b) Image from side

Figure 3. Field images of Bitter gourd

3. COLLISION DETECTION TECHNIQUE

To perform agricultural operations, the redundant manipulator must avoid collisions with the surroundings. Collisions can be detected by the bounding box technique [30]. In the present study, different vegetables and guava fruits are considered as task-space locations for picking/plucking operations. Trellis, tree trunks, and branches are considered as the obstacles. These obstacles need to be bound by the 3D bounding box. The solid boundaries of each object are represented by a set of points. From this set of points, the extremum coordinates of points are found. These extremum coordinates are used to find the vertices of the bounding box using a convex hull algorithm, the facet information (i.e., the vertices which are used to form a particular face) is calculated. Finally, a 3D bounding box is modelled around each obstacle using facets and their corresponding vertices as shown in Figure 4. Whenever a particular configuration of manipulator links lies within this bounding box, a collision can be detected. The collision detection algorithm is stated in Table 3. To implement the algorithm for convex and concave-shaped obstacles, the obstacle can be enveloped by using several small bounding boxes. So this algorithm can be effectively implemented to different complex-shaped obstacles.

TABLE 3. Collision detection algorithm

Algorithm: Collision detection

1. Input: bounding box extremum coordinates.

$x_{min}, y_{min}, z_{min}, x_{max}, y_{max}, z_{max}$ and point $p_i(p_{ix}, p_{iy}, p_{iz})$

2. Collision condition:

for $i = 1:n$

if $x_{min} <= p_{ix} <= x_{max}$ && $y_{min} <= p_{iy} <= y_{max}$

&& $z_{min} <= p_{iz} <= z_{max}$

collision with obstacle

else

no collision with the obstacle

end

end

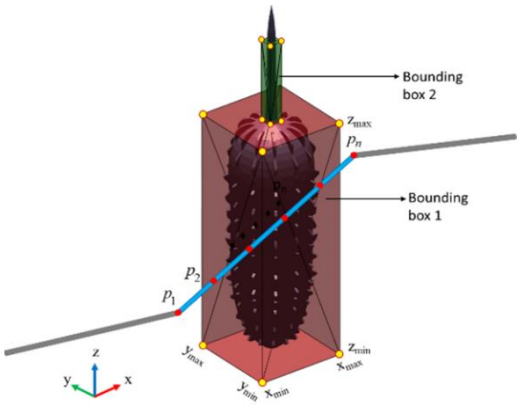

(a) 3D view

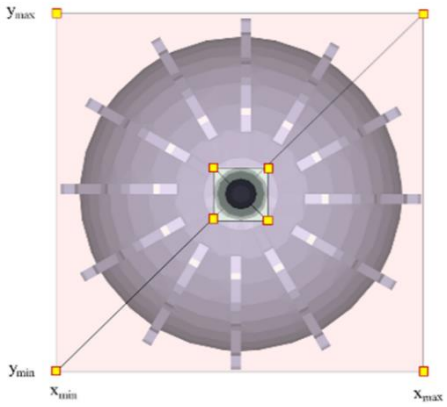

(b) top view

Figure 4. Object encompassed by a bounding box

For detecting a collision with obstacles, a set of uniformly distributed points $p_1, p_2, \ldots, p_n$ on each link of the manipulator, and extremum points of the bounding boxes are considered. Each point on the manipulator is taken as a query point 'q' and a check will be performed with bounding box extremum points. Whenever the query point lies within the bounding box, a collision is detected between the manipulator and the obstacle. The configuration that leads to collisions has been determined using the aforesaid approach and these configurations should be avoided.

To eliminate the configuration that causes a collision with the environment, a penalty approach has been implemented during the calculation of IK for robot manipulator.

4. OPTIMIZATION AND PROBLEM FORMULATION

To obtain the joint variables, the IK problem of the redundant manipulator is formulated using classical optimization technique at the joint position level. this approach was easily applied to any redundant manipulators with a different configuration.

4. 1 Objective Function The objective function is the manipulator's reachability. This is can be measured as the total cumulative error in Euclidean distances and Euler angles, that is, the error in the position and orientation of the manipulator's end-effector to reach the intended task space locations. A schematic diagram of a general serial redundant manipulator is shown in Figure 5. In cartesian coordinates, the position error can be expressed as:

$$P_{error} = (x_d - x_a)^2 + (y_d - y_a)^2 + (z_d - z_a)^2 \quad (4)$$

In Equation (4), (x_d, y_d, z_d) and (x_a, y_a, z_a) are vectors that correspond to desired (r_d) and actual (r_a) positions respectively.

Similarly, orientation error can be expressed as:

$$O_{error} = (\alpha_d - \alpha_a)^2 + (\beta_d - \beta_a)^2 + (\gamma_d - \gamma_a)^2 \quad (5)$$

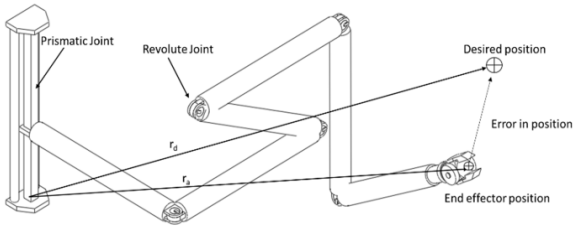

Figure 5. Schematic diagram of a serial redundant manipulator

In the above, Equation (5), $(\alpha_d, \beta_d, \gamma_d)$ and $(\alpha_a, \beta_a, \gamma_a)$ are Euler angles corresponding to desired and actual orientations respectively in relation with base frame.

To compute the cartesian coordinates of the end-effector's position in terms of the D-H parameters, $[a, \alpha, d, \theta]$, the conventional forward kinematics method is utilized.

As a result, the objective function can be defined as the sum of the cumulative errors of position and orientations. Finally, the objective function can be expressed in Equation (6):

Minimize:

$$f = [(x_{id} - x_{ia})^2 + (y_{id} - y_{ia})^2 + (z_{id} - z_{ia})^2 + (\alpha_{id} - \alpha_{ia})^2 + (\beta_{id} - \beta_{ia})^2 + (\gamma_{id} - \gamma_{ia})^2] \quad (6)$$

From the above equation, a suitable configuration for the manipulator was obtained. But to get a collision-free configuration for the manipulator, penalties are imposed in the objective function. The modified objective function for the IK problem is given in Equation 6. Due to this penalty, the objective function is again run (search) for minimization.

$$\text{Minimize: } f = [(x_{id} - x_{ia})^2 + (y_{id} - y_{ia})^2 + (z_{id} - z_{ia})^2 + (\alpha_{id} - \alpha_{ia})^2 + (\beta_{id} - \beta_{ia})^2 + (\gamma_{id} - \gamma_{ia})^2] + \sum_{i=1}^{m} C_i \quad (7)$$

where C_i is the i^{th} penalty when there is a collision and m is the number of collisions.

4. 2 Constraints due to Limiting Values of D-H Parameters The DH parameters of the linkages are constrained. These are imposed as limitations on the optimization technique.

In this study, one of the joints is prismatic and the remaining are revolute. As a corollary, the joint variable for each link, say q, would be either d (for prismatic) or θ (for revolute). Constraints on the DH parameters for the i^{th} link can be expressed in the following manner given in Equation (8):

$$\begin{cases} a_{il} \le a_i \le a_{iu}, \\ \alpha_{il} \le \alpha_i \le \alpha_{iu}, \\ d_{il} \le d_i \le d_{iu} \text{ if the joint is prismatic,} \\ \theta_{il} \le \theta_i \le \theta_{iu} \text{ if the joint is revolute,} \\ q_{il} \le q_i \le q_{iu} \quad \forall j \end{cases} \quad (8)$$

where $i = 1, 2, \ldots, n$; l in suffix represents lower bound while u represents the upper bound.

In the present study, joint variable limits are presented in Equation (9).

$$\begin{cases} 0 \le d_1 \le 20cm & \text{for Prismatic joint,} \\ -180 \le \theta_i \le 180 & \text{if the joint is revolute for i=2,3,..6.,} \\ -90 \le \theta_i \le 90 & \text{if the joint is revolute for i=7,8,9} \end{cases} \quad (9)$$

4. 3. Optimization Technique To solve the objective function with constraints we used one of the classical optimization methods i.e., 'Sequential Quadratic Programming (SQP) technique'**. SQP method is the most advanced nonlinear programming technique. SQP is a quadratic approximation of the Lagrangian function with constraints linearization. To get the search direction, a quadratic subproblem is formulated and solved. A modified BFGS formula is used to update the Hessian matrix during the line search, which can be done with two alternative merit functions. By using this approach, simulations are carried out in the present study. This algorithm gives the optimum values at local minima. The problem of trapping at local minima can be overcome by considering multiple initial guesses from different start points, which can be known as the "multi-start technique", and it can be easily extended to a global minimum problem.

5. RESULTS AND DISCUSSION

In this section, results of IK simulations for robot operating in different agricultural environments are presented. Three different virtual environments are modelled which depicts the real-time environment in the agricultural field. Simulations of the robot are carried out in this modelled environment. For fruit/ vegetable picking operations, a redundant robot with nine links and 9-DOF is considered. The first six links are of uniform length, with 20 cm each in a cylindrical shape with 2cm diameter. The last 3 links constitute the wrist, which allows the end-effector to place in the desired orientation. The IK solutions for the redundant robot manipulator are computed using optimization technique as discussed in section 4. The collision detection technique was implemented and extended to cylindrical links for avoiding obstacles like tree trunks and branches, as discussed in section 3 using Equation (6). To determine the collision between the cylindrical links and obstacles, the surface of the link is considered as a series of circles. If any coordinates of these circles are lies within the bounding box, a collision can be detected by using the algorithm discussed in section 3. A constant value of penalty is added to the objective function for all cases of simulations. The penalty value can be determined based on the merit function which was used as the objective of the optimization. The penalty value is taken as 100 for the simulation of a redundant manipulator in the agricultural environment.

Configuration of robot manipulator during the simulation was plotted in Matlab. However, it is not possible to show the orientation of the manipulator in a Matlab environment. So, here the orientation was presented using Simscape Multibody in the Simulink environment. To represent in Simulink environment, the robot is modelled in Solidworks and saved in Unified Robotic Description Format (URDF) file format, by describing the robot's physical contacts and joint locations. In the Simulink environment, the model was shown as a number of blocks as depicted in Figure 6. To show the agricultural environment, different virtual 3D models were added using the *'file solid'* block. For identifying the position of the end-effector a *'transformation sensor'* was added at wrist and same data is exported to Matlab workspace through *'PS- Simulink Converter'*. This environment was saved in.*slx* file. format.

In the present work, we considered three different agricultural fields namely: Bitter gourd, Tindora, and Guava garden. These fields are modelled in Solidworks which resembles real environments. Task-space locations are identified from the image, using mapping technique as mentioned in section 2.3, coordinates of the task-space location in real-world were determined.

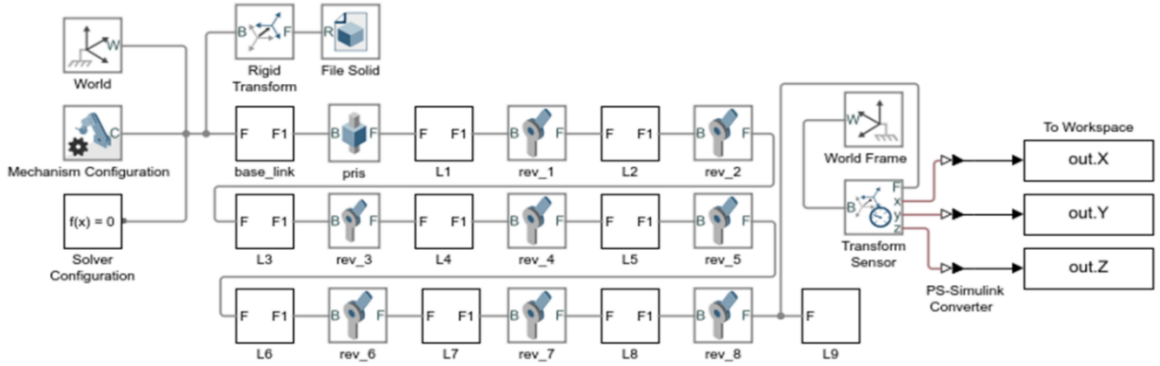

Figure 6. Simulink environment of 9 DOF robot

5. 1. Case Studies

Application 1: Bitter Gourd:

Figure 7 shows the virtual environment of Bitter gourd plants. Here Bitter gourd is to be harvested and several obstacles such as leaves, stems, and trellis could be avoided for collision-free travel (configuration) of the manipulator. In the cluttered environment, the robot is directed to move from one task space location to another task space location by avoiding obstacles. Collisions with obstacles can be avoided by bounding box criteria as mentioned in section 3. Using the numerical method, IK for redundant manipulator determined as discussed in section 4, and configuration was plotted to reach (42,36,60) mm location in the environment, as shown in Figure 8. Figure 9 shows the robot manipulator moving from one task space location (38, 34, 60) to another task space location (59, -15, 60) by avoiding obstacles in between them. The IK solutions at different locations are presented in Table 4.

The computational time for attaining an IK solution of the redundant manipulator in a cluttered environment is about 54 seconds, which is less when compared to evolutionary algorithms [34]. For all cases, the positional error is very small. The configuration and orientation of the manipulator for one task-space location are shown in Figure 10 using Simscape Multibody. The error values during simulations were compared with existing

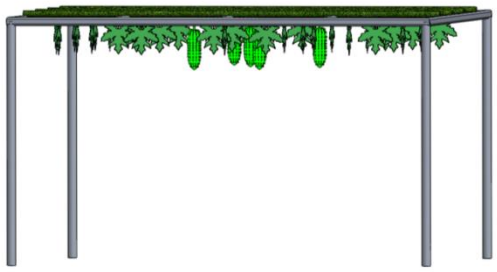

Figure 7. Solidworks model of Bitter gourd environment

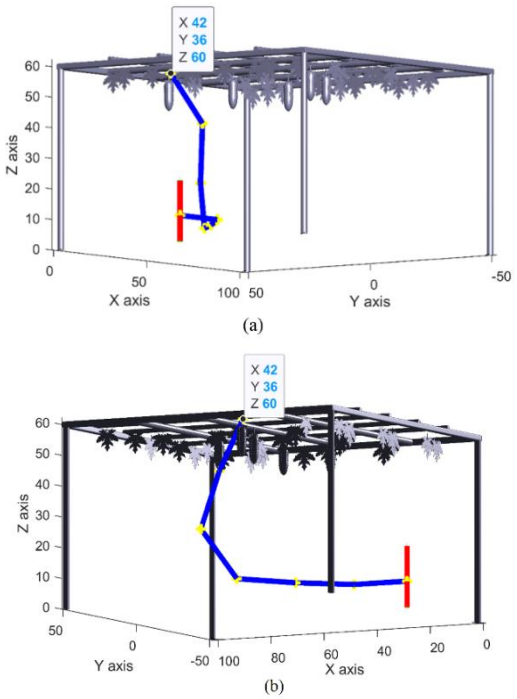

Figure 8. Robot configuration in different views at task location (42,36,60)

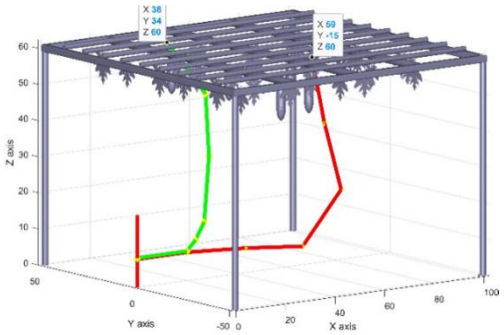

Figure 9. Manipulator configuration for different task space locations: (38,34,60) and (59,- 15,60)

TABLE 4. Joint variables for different task space locations

S. No	Task space locations		Joint variables									Error
	Position (cm)	Orientation (degrees)	(cm)	(degrees)								
			q_1	θ_1	θ_2	θ_3	θ_4	θ_5	θ_6	θ_7	θ_8	
1	(38,34,60)	(-26,12,34)	8.16	44.57	5.33	50.95	56.99	-35.41	6.34	221.30	50.87	1.13e-07
2	(43.25,29.25,55)	(-10,5,23)	8.12	35.38	-4.73	55.25	66.34	-31.29	1.50	-131.07	43.13	6.79e-08
3	(48.5,24.5,50)	(-30,-40,20)	8.14	27.85	-16.29	58.61	74.69	-24.68	1.50	30.30	21.22	2.11e-07
4	(53.75,19.75,55)	(-22,14,33)	8.15	21.76	-9.88	55.08	67.54	-16.94	1.50	-29.89	-33.31	1.38e-07
5	(59,15,60)	(30,16,22)	7.91	15.60	-2.06	50.47	58.72	-11.41	13.43	13.45	34.23	1.50e-07
6	(59,-15,60)	(23,43,17)	7.84	-15.58	-1.90	50.38	58.62	11.46	11.76	33.71	23.54	1.49e-07

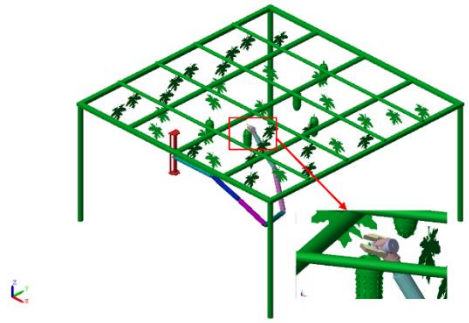

Figure 10. Configuration and orientation of manipulator for given task space location in Bitter gourd environment

literature. It is observed that for ten link manipulators optimized function value (error value) is 0.0036 [35]. In present studies, the error values are negligible (10^{-7} to 10^{-8} times) compared to the positional error in literature, which is almost zero and ensures that the end-effector reaches the desired target precisely.

Application 2: Tindora: The virtual environment of Tindora plants is shown in Figure 11. Configuration of robot for reaching the location of (59.25,37,57) is plotted in Figure 12. Error during the IK solution is in order of 10^{-8}, which shows a minimal positional error of the manipulator. For better visibility of orientation, 3D model of robot in the virtual environment using Simscape shown in Figure 13 along with the orientation of end-effector.

Application 3: Guava: A 3D environment of guava plants is modeled and presented in Figure 14. The robot is directed to move from (49,69,62) task-space location to (57, -67, 60) via some intermediate task-space locations. All these configurations are plotted as shown in Figure 15. 3D model of the robot along with orientation is depicted in Figure 16.

5. 2. Joint Trajectory with Simulation Study

Joint variables are calculated for particular task-space locations as discussed in section 4. In this section, a simulation study is performed to identify the position, velocity, and acceleration of joints with respect to time period, during robot motion. To perform the simulation study in a *Simscape* environment, it is required to add step input for each joint by specifying targeted values. The position, velocity, and acceleration of each joint are

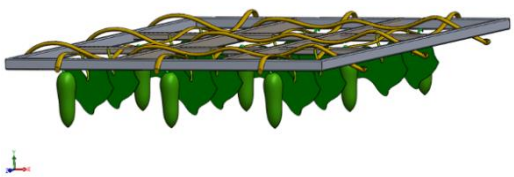

Figure 11. 3D model of Tindora environment in Solidworks

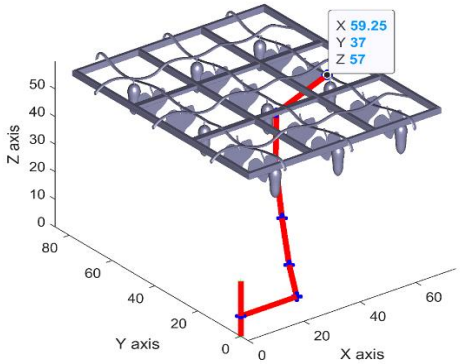

Figure 12. Manipulator configuration at task location of (59.25,37,57)

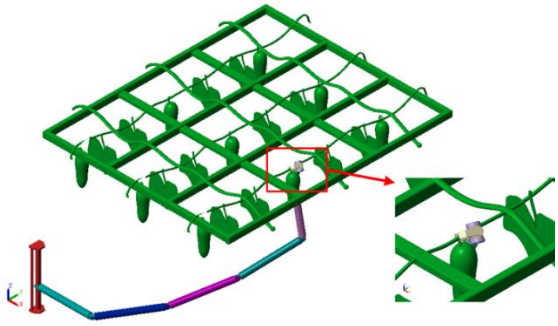

Figure 13. Configuration and orientation of manipulator for given task space location in Bitter gourd environment

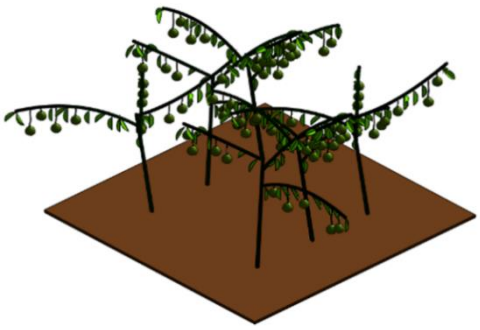

Figure 14. 3D model of Guava environment

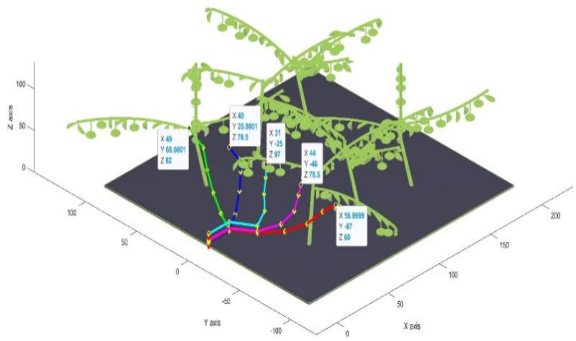

Figure 15. Different configurations of manipulator in Matlab environment

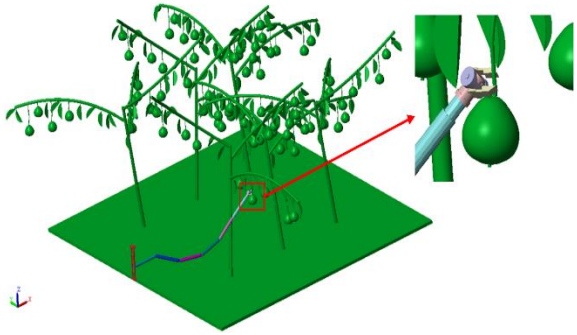

Figure 16. Configuration and orientation of manipulator for given task space location in guava environment

sensed and viewed in the scope box. Also, the location of end-effector is sensed by the *transform sensor*. For understanding of the Simulink model, a block diagram of the last joint is presented in Figure 17.

A simulation study is performed for 0.01 second. During the simulation of the manipulator, each joint variable with respect to time is presented in Figure 18. During simulations, all joints are directed to move from zero position to targeted position. Figure 18(a) shows the change in positions of all 9 joints. From the figure, it is observed that all joints are beginning at zero position, when time proceeds, joint positional values are uniformly increasing to reach the final position. Figure 18(b) shows the variation of velocities. Initially, there is an increase in velocities up to some period of time and then reaches the maximum value. Constant velocity profile was followed after reaching maximum values. Figure 18(c) shows the variations in accelerations. Accelerations of each joint is started at zero and there is a raise in up to some time period, after that there is a smooth decrement to reach zero without jerks during the simulation.

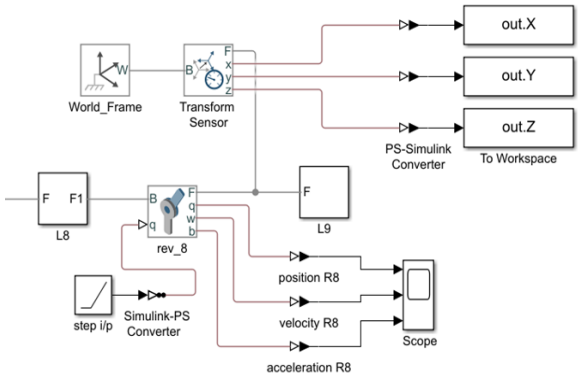

Figure 17. Block diagram for wrist location in Simulink environment

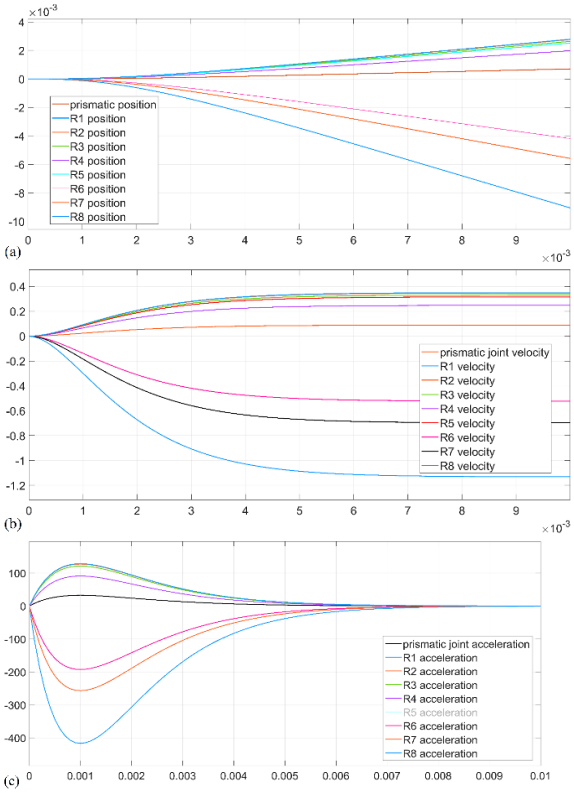

Figure 18. Variation of Joint variables at different time period (a) position (b) velocity (c) acceleration profiles

6. CONCLUSIONS

This article presented the kinematic design of a redundant agricultural harvesting manipulator. This redundant manipulator is intended to be used for different agricultural tasks in the harvesting of crops like Bitter gourd, tindora, and guava. The manipulator has to access the plant from any direction by avoiding collision with obstacles. To access the plant, a configuration of the robot was obtained by inverse kinematics. IK problem was formulated as a nonlinear optimization problem. A classical nonlinear optimization SQP method was used to find the joint variables along with the obstacle avoiding technique. The collision avoidance technique was implemented using a bounding box approach by including a collision detection algorithm. The results demonstrate that the IK solution was accurate. The joint trajectories of the robot while reaching desired task-space location has been depicted using Simscape Multibody. Smooth joint trajectories corresponding to motion were attained during the simulation. The study can be extended to optimal design of manipulator along with an increased number of degrees of freedom at joints and dynamic control of the robot manipulator.

7. REFERENCES

1. Silwal, A., Davidson, J.R., Karkee, M., Mo, C., Zhang, Q. and Lewis, K., "Design, integration, and field evaluation of a robotic apple harvester", ***Journal of Field Robotics***, Vol. 34, No. 6, (2017), 1140-1159, doi: 10.1002/rob.21715
2. Edan, Y., Han, S. and Kondo, N., "Automation in agriculture", Springer handbook of automation, (2009), 1095-1128, doi: 10.1007/978-3-540-78831-7_63
3. Pedersen, S.M., Fountas, S., Have, H. and Blackmore, B., "Agricultural robots—system analysis and economic feasibility", ***Precision Agriculture,*** Vol. 7, No. 4, (2006), 295-308, doi: 10.1007/s11119-006-9014-9
4. Belforte, G., Deboli, R., Gay, P., Piccarolo, P. and Aimonino, D.R., "Robot design and testing for greenhouse applications", ***Biosystems Engineering***, Vol. 95, No. 3, (2006), 309-321, doi: 10.1016/j.biosystemseng.2006.07.004
5. Hayashi, S., Shigematsu, K., Yamamoto, S., Kobayashi, K., Kohno, Y., Kamata, J. and Kurita, M., "Evaluation of a strawberry-harvesting robot in a field test", ***Biosystems Engineering***, Vol. 105, No. 2, (2010), 160-171, doi: 10.1016/j.biosystemseng.2009.09.011
6. Bechar, A. and Vigneault, C., "Agricultural robots for field operations: Concepts and components", ***Biosystems Engineering***, Vol. 149, (2016), 94-111, doi: 10.1016/j.biosystemseng.2016.06.014
7. Kootstra, G., Wang, X., Blok, P.M., Hemming, J. and Van Henten, E., "Selective harvesting robotics: Current research, trends, and future directions", ***Current Robotics Reports***, Vol. 2, No. 1, (2021), 95-104, doi: 10.1007/s43154-020-00034-1
8. Maciejewski, A.A. and Klein, C.A., "Obstacle avoidance for kinematically redundant manipulators in dynamically varying environments", ***The International Journal of Robotics Research***, Vol. 4, No. 3, (1985), 109-117, doi: 10.1177/027836498500400308
9. Korayem, M.H., Ahmadi, R., Jafari, N., Jamali, Y., Kioumarsi, M. And Habibnezhad, A., "Design, modeling, implementation and experimental analysis of 6r robot (technical note)", ***International Journal of Engineering, Transactions A: Basics,*** Vol. 21, No. 1, (2008), 71-84.
10. Craig, J.J., "Introduction to robotics: Mechanics and control, Pearson Educacion, (2005), ISBN-13: 9781292040042
11. Aristidou, A. and Lasenby, J., "Inverse kinematics: A review of existing techniques and introduction of a new fast iterative solver", University of Cambridge Technical Report, (2009) CUED/F-INFENG/TR-632.
12. Goldenberg, A.A. and Lawrence, D.L., "A generalized solution to the inverse kinematics of robotic manipulators", ***Journal of Dynamic Systems, Measurement, and Control***, Vol. 107, No. 1, (1985), 103-106, doi: 10.1115/1.3140699
13. Kumar, S., Sukavanam, N. and Balasubramanian, R., "An optimization approach to solve the inverse kinematics of redundant manipulator", ***International Journal of Information and System Sciences (Institute for Scientific Computing and Information)***, Vol. 6, No. 4, (2010), 414-423.
14. Bagheri, A., Narimanzadeh, N., Siavash, A.S. And Khoobkar, A.R., "Gmdh type neural networks and their application to the identification of the inverse kinematics equations of robotic manipulators (research note)", ***International Journal of Engineering***, Vol. 18, No. 2, (2005), 135-143.
15. Whitney, D.E., "Resolved motion rate control of manipulators and human prostheses", ***IEEE Transactions on man-machine systems***, Vol. 10, No. 2, (1969), 47-53, doi: 10.1109/TMMS.1969.299896
16. Chembuly, V.S. and Voruganti, H.K., "An optimization based inverse kinematics of redundant robots avoiding obstacles and singularities", in Proceedings of the Advances in Robotics. (2017), 1-6, doi: 10.1145/3132446.3134888
17. Zhao, Y., Gong, L., Huang, Y. and Liu, C., "A review of key techniques of vision-based control for harvesting robot", ***Computers and Electronics in Agriculture***, Vol. 127, (2016), 311-323, doi: 10.1016/j.compag.2016.06.022
18. Hartley, R.I. and Sturm, P., "Triangulation", ***Computer Vision and Image Understanding***, Vol. 68, No. 2, (1997), 146-157, doi: 10.1006/cviu.1997.0547
19. Van Henten, E., Schenk, E., Van Willigenburg, L., Meuleman, J. and Barreiro, P., "Collision-free inverse kinematics of the redundant seven-link manipulator used in a cucumber picking robot", ***Biosystems Engineering***, Vol. 106, No. 2, (2010), 112-124, doi: 10.1016/j.biosystemseng.2010.01.007
20. Buemi, F., Massa, M., Sandini, G. and Costi, G., "The agrobot project", ***Advances in Space Research***, Vol. 18, No. 1-2, (1996), 185-189, doi: 10.1016/0273-1177(95)00807-Q
21. Khatib, O., Real-time obstacle avoidance for manipulators and mobile robots, in Autonomous robot vehicles. 1986, Springer.396-404, doi: 10.1007/978-1-4613-8997-2_29
22. Korayem, M., Nazemizadeh, M. and Azimirad, V., "Optimal trajectory planning of wheeled mobile manipulators in cluttered environments using potential functions", ***Scientia Iranica***, Vol. 18, No. 5, (2011), 1138-1147, doi: 10.1016/j.scient.2011.08.026
23. Korayem, M., Nazemizadeh, M. and Rahimi, H., "Trajectory optimization of nonholonomic mobile manipulators departing to a moving target amidst moving obstacles", ***Acta Mechanica***, Vol. 224, No. 5, (2013), 995-1008, doi: 10.1007/s00707-012-0799-5
24. Korayem, M.H., Nazemizadeh, M. and Nohooji, H.R., "Optimal point-to-point motion planning of non-holonomic mobile robots in the presence of multiple obstacles", ***Journal of the Brazilian Society of Mechanical Sciences and Engineering***, Vol. 36, No. 1, (2014), 221-232, doi: 10.1007/s40430-013-0063-5
25. Tang, Z., Xu, L., Wang, Y., Kang, Z. and Xie, H., "Collision-free motion planning of a six-link manipulator used in a citrus picking robot", ***Applied Sciences***, Vol. 11, No. 23, (2021), 11336, doi: 10.3390/app112311336
26. Koren, Y. and Borenstein, J., "Potential field methods and their inherent limitations for mobile robot navigation", in ICRA. Vol. 2, (1991), 1398-1404, doi: 10.1109/ROBOT.1991.131810
27. Gottschalk, S., Lin, M.C. and Manocha, D., "Obbtree: A hierarchical structure for rapid interference detection", in Proceedings of the 23rd annual conference on Computer graphics and interactive techniques. (1996), 171-180, doi: 10.1145/237170.237244
28. Barequet, G. and Har-Peled, S., "Efficiently approximating the minimum-volume bounding box of a point set in three dimensions", ***Journal of Algorithms***, Vol. 38, No. 1, (2001), 91-109, doi: 10.1006/jagm.2000.1127
29. Held, M., Klosowski, J.T. and Mitchell, J.S., "Evaluation of collision detection methods for virtual reality fly-throughs", in Canadian Conference on Computational Geometry, Citeseer. (1995), 205-210.
30. Chembuly, V. and Voruganti, H.K., "An efficient approach for inverse kinematics and redundancy resolution of spatial redundant robots for cluttered environment", ***SN Applied Sciences***, Vol. 2, No. 6, (2020), 1-20, doi: 10.1007/s42452-020-2825-x
31. Bac, C.W., Van Henten, E.J., Hemming, J. and Edan, Y., "Harvesting robots for high-value crops: State-of-the-art review and challenges ahead", ***Journal of Field Robotics***, Vol. 31, No. 6, (2014), 888-911, doi: 10.1002/rob.21525
32. Tinoco, V., Silva, M.F., Santos, F.N., Rocha, L.F., Magalhães, S. and Santos, L.C., "A review of pruning and harvesting

manipulators", in 2021 IEEE International Conference on Autonomous Robot Systems and Competitions (ICARSC), IEEE. (2021), 155-160, doi: 10.1109/ICARSC52212.2021.9429806

33. Wu, Y., Tang, F. and Li, H., "Image-based camera localization: An overview", ***Visual Computing for Industry, Biomedicine, and Art,*** Vol. 1, No. 1, (2018), 1-13, doi: 10.1186/s42492-018-0008-z
34. Tabandeh, S., Melek, W.W. and Clark, C.M., "An adaptive niching genetic algorithm approach for generating multiple solutions of serial manipulator inverse kinematics with applications to modular robots", ***Robotica***, Vol. 28, No. 4, (2010), 493-507, doi: 10.1017/S0263574709005803
35. Singla, E., Tripathi, S., Rakesh, V. and Dasgupta, B., "Dimensional synthesis of kinematically redundant serial manipulators for cluttered environments", ***Robotics and Autonomous Systems***, Vol. 58, No. 5, (2010), 585-595, doi: 10.1016/j.robot.2009.12.005

Persian Abstract

چکیده

این مقاله یک تکنیک مبتنی بر بهینه‌سازی را برای حل سینماتیک معکوس (IK)دستکاری‌کننده‌های اضافی فضایی در محیط‌های کشاورزی (فضاهای کاری) ارائه می‌کند. یک پیکربندی سینماتیکی با ۹ درجه آزادی (DOF)با هشت چرخش و یک مفصل منشوری برای بهبود دسترسی در فضاهای کاری پیچیده مدل‌سازی شده است. دستکاری کننده پیشنهادی برای برداشت میوه ها و سبزیجات شبیه سازی شده است. برای انجام کار مورد نظر در محیط کاری نیاز است که راه حل IK ربات مشخص شود. مسئله IK به عنوان یک مسئله بهینه سازی محدود با هدف به حداقل رساندن خطاهای موقعیتی و جهت گیری با اجتناب از موانع فرموله شده است. یک محیط CAD سه بعدی با گیاهان مختلف میوه و سبزیجات در Solidworks مدل سازی شده است. یک مکان هدف در این محیط برای چیدن میوه/سبزیجات انتخاب شده است. تنه، شاخه ها و برگ ها به عنوان انسداد در نظر گرفته می شوند. تکنیک اجتناب از برخورد با استفاده از رویکرد جعبه مرزی با گنجاندن یک الگوریتم تشخیص برخورد اجرا شد. شبیه‌سازی‌های IK از دستکاری‌کننده اضافی فضایی در یک محیط بهم ریخته انجام شد و نتایج گزارش شد. مسیرهای مشترک ربات در حین رسیدن به مکان فضای کاری مورد نظر با استفاده از Simscape Multibody به تصویر کشیده شده است. نتایج نشان می‌دهد که عامل پایانی ربات با یک راه‌حل دقیق IK با موفقیت به محل کار مورد نظر رسیده است. این رویکرد در طیف گسترده ای از محیط های کاری بر اساس نتایج شبیه سازی راه حل IK ربات ها سازگار است.